Biomedicine & Pharmacotherapy 102 (2018) 481–493

Contents lists available at ScienceDirect

Biomedicine & Pharmacotherapy

journal homepage: www.elsevier.com/locate/biopha

The novel piperazine-containing compound LQFM018: Necroptosis cell death mechanisms, dopamine D_4 receptor binding and toxicological assessment

Fabiana Bettanin Costa[a,1], Alane P. Cortez[a,1], Renato Ivan de Ávila[a], Flávio S. de Carvalho[a], Wanessa M. Andrade[a], Andrezza F. da Cruz[a], Karinna B. Reis[b], Ricardo Menegatti[b], Luciano M. Lião[c], Luiz Antônio S. Romeiro[d,e], François Noël[f], Carlos Alberto M. Fraga[g], Eliezer J. Barreiro[g], Germán Sanz[h], Marcella F. Rodrigues[h], Boniek G. Vaz[h], Marize Campos Valadares[a,*]

[a] Laboratório de Farmacologia e Toxicologia Celular - FarmaTec, Faculdade de Farmácia, Universidade Federal de Goiás, Goiânia, GO, Brazil
[b] Laboratório de Química Farmacêutica Medicinal (LQFM), Faculdade de Farmácia, Universidade Federal de Goiás, Goiânia, GO, Brazil
[c] Laboratório de Ressonância Magnética Nuclear, Instituto de Química, Universidade Federal de Goiás, Goiânia, GO, Brazil
[d] Universidade Católica de Brasília, Brasília, DF, Brazil
[e] Universidade de Brasília, Brasília, DF, Brazil
[f] Laboratório de Farmacologia Bioquímica e Molecular, Instituto de Ciências Biológicas, Universidade Federal do Rio de Janeiro, Rio de Janeiro, RJ, Brazil
[g] Laboratório de Avaliação e Síntese de Substâncias Bioativas (LASSBio), Faculdade de Farmácia, Universidade Federal do Rio de Janeiro, Rio de Janeiro, RJ, Brazil
[h] Laboratório de Cromatografia e Espectrometria de Massas (LaCEM), Instituto de Química, Universidade Federal de Goiás, Goiânia, GO, Brazil

ARTICLE INFO

Keywords:
Antileukemic activity
Chronic myeloid leukemia
Piperazine
Necroptosis
Regulated necrosis

ABSTRACT

Piperazine is a promising scaffold for drug development due to its broad spectrum of biological activities. Based on this, the new piperazine-containing compound LQFM018 (**2**) [ethyl 4-((1-(4-chlorophenyl)-1H-pyrazol-4-yl) methyl)piperazine-1-carboxylate] was synthetized and some biological activities investigated. In this work, we described its ability to bind aminergic receptors, antiproliferative effects as well as the LQFM018 (**2**)-triggered cell death mechanisms, in K562 leukemic cells, by flow cytometric analyses. Furthermore, acute oral systemic toxicity and potential myelotoxicity assessments of LQFM018 (**2**) were carried out. LQFM018 (**2**) was originally obtained by molecular simplification from LASSBio579 (**1**), an analogue compound of clozapine, with 33% of global yield. Binding profile assay to aminergic receptors showed that LQFM018 (**2**) has affinity for the dopamine D_4 receptor (K_i = 0.26 μM). Moreover, it showed cytotoxicity in K562 cells, in a concentration and time-dependent manner; IC_{50} values obtained were 399, 242 and 119 μM for trypan blue assay and 427, 259 and 50 μM for MTT method at 24, 48 or 72 h, respectively. This compound (427 μM) also promoted increase in LDH release and cell cycle arrest in G2/M phase. Furthermore, it triggered necrotic morphologies in K562 cells associated with intense cell membrane rupture as confirmed by Annexin V/propidium iodide double-staining. LQFM018 (**2**) also triggered mitochondrial disturb through loss of ΔΨm associated with increase of ROS production. No significant accumulation of cytosolic cytochrome c was verified in treated cells. Furthermore, it was verified an increase of expression of TNF-R1 and mRNA levels of CYLD with no involvement in caspase-3 and -8 activation and NF-κB in K562 cells. LQFM018 (**2**) showed *in vitro* myelotoxicity potential, but it was orally well tolerated and classified as UN GHS category 5 (LD_{50} > 2000–5000 mg/Kg). Thus, LQFM018 (**2**) seems to have a non-selective action considering hematopoietic cells. In conclusion, it is suggested LQFM018 (**2**) promotes cell death in K562 cells *via* necroptotic signaling, probably with involvement of dopamine D_4 receptor. These findings open new perspectives in cancer therapy by use of necroptosis inducing agents as a strategy of reverse cancer cell chemoresistance.

* Corresponding author at: Faculdade de Farmácia – Universidade Federal de Goiás, Rua 240 esquina com 5ª Avenida, s/n, Setor Universitário, Goiânia, GO, Brazil.
E-mail address: marizecv@ufg.br (M.C. Valadares).
[1] These authors equally contributed to this study.

https://doi.org/10.1016/j.biopha.2018.02.120
Received 30 October 2017; Received in revised form 21 February 2018; Accepted 23 February 2018

1. Introduction

Piperazine is a promising scaffold for drug development [1] due to its broad spectrum of biological activities [2]. It is present in a large variety of commercially available anticancer drugs such as imatinib mesylate, a tyrosine kinase inhibitor (TKI) that acts by inhibiting specific tyrosine kinases, such as BCR-ABL fusion oncoprotein in chronic myeloid leukemia [3–5].

Chronic myeloid leukemia is a myeloproliferative disorder characterized by the neoplastic transformation of hematopoietic stem cells in the bone marrow and their accumulation in the bloodstream. Its molecular hallmark is the Philadelphia chromosome (Ph), an aberrant fusion gene originated by translocation between chromosomes 9 and 22 which results in a chimeric gene product BCR-ABL [6–8]. The mutations of Ph and overexpression of BCR-ABL oncoprotein can promote resistance to apoptosis induced by conventional chemotherapy, and make chronic myeloid leukemia stem cells capable of escaping from imatinib and other TKI agents [9–12]. Therefore, compounds which also promote other or additional cellular death mechanisms, such as regulated necrosis, could be a new therapeutic option.

In accordance with the Nomenclature Committee on Cell Death (NCCD), regulated cell death occurs as part of physiological programs or can be activated once adaptive responses to perturbations of the extracellular or intracellular microenvironment fail [13,14]. Regulated necrosis, in turn, plays a major role in both physiological scenarios (*e.g.* embryonic development) and pathological settings (*e.g.* ischemic disorders); various types have been characterized, including necroptosis, mitochondrial permeability transition (MPT)-dependent regulated necrosis and parthanatos ([15–18]).

Currently, studies show that necrosis is a regulated process involving a set of transduction pathways and degradative mechanisms [19–21]. In view of that, the term “necroptosis” can be defined as a receptor interacting protein kinase 3 (RIPK3)-dependent molecular cascade promoting regulated necrosis [13]. Necrosis can be characterized by cell volume gain, organelle swelling, plasma membrane rupture and loss of intracellular content, which can lead to inflammation [22,23]. The cellular signaling that triggers necrosis is complex and requires different molecules working in concert. This process can be initiated by death receptors such as the tumor necrosis factor (TNF) receptor family, including TNF, Fas and TNF-related apoptosis-inducing ligand (TRAIL) [24].

Considering this background, this study describes the synthesis of the new piperazine-containing compound LQFM018 (**2**) [ethyl 4-((1-(4-chlorophenyl)-1H-pyrazol-4-yl)methyl)piperazine-1-carboxylate], a closely related analogue of LASSBio579 (**1**), a compound obtained by molecular simplification of atypical antipsychotic clozapine [25]. Moreover, the LQFM018 (**2**)-triggered cell death mechanisms in K562 cells as well as acute oral systemic toxicity and potential myelotoxicity assessments of LQFM018 (**2**) were carried out.

2. Materials and methods

2.1. Chemicals

An *In Vitro* Lactate Dehydrogenase Activity Assay kit, a Caspase-3 Colorimetric Assay kit, Dulbecco’s modified Eagle’s medium (DMEM), Roswell Park Memorial Institute (RPMI)-1640 medium, gentamycin, amphotericin B, propidium iodide (PI), RNAse, acetate 2,7-dichlorofluorescein (DCFH-DA), EDTA, bovine serum albumin (BSA), phosphatidylcholine, sodium taurodeoxycholate hydrate, rhodamine 123, granulocyte-macrophage colony-stimulating factor (GM-CSF), 3-[4,5-dimethylthiazol-2-yl]-2,5-diphenyl tetrazolium bromide (MTT) and ethidium bromide were purchased from Sigma-Aldrich (St. Louis, MO, USA). A CaspaTagTM Caspases-8 *In Situ* Assay kit was obtained from Millipore^{TM} (Temecula, CA, USA). Fetal bovine serum (FBS) and acetic acid were acquired from Gibco (Grand Island, NY, USA) and Cromoline (Diadema, SP, Brazil), respectively. Trypan blue dye, dimethyl sulfoxide (DMSO), ethanol, methanol and Triton X-100 were obtained from Vetec (Rio de Janeiro, RJ, Brazil), while May-Grünwald-Giemsa dye was purchased from Merck (Darmstadt, HE, Germany). Hoechst 33342 dye was acquired from Invitrogen (GrandIsland, NY, USA). Xylasine and ketamine hydrochloride were obtained from Syntec (Cotia, SP, Brazil) and König (Embu-Guaçu, SP. Brazil), respectively. Agar and an FITC Annexin V Apoptosis Detection kit were purchased from BD Bioscience (Franklin Lakes, NJ, USA). The mouse monoclonal anti-human cytochrome c (6H2, sc-13561 PE) and anti-human tumor necrosis factor receptor 1 (TNF-R1) (6A658, sc-73195 FITC) antibodies were acquired from Santa Cruz Biotechnology (Dallas, TX, USA). RNeasy mini, QuantiTect Reverse Transcription, Rotor-Gene SYBR Green PCR and QuantiTect Reverse Transcription kits were purchased from Qiagen (Hilden, Germany). The sunflower oil was obtained from Bunge Alimentos (Gaspar, SC, Brazil).

2.2. Cell cultures

Balb/c 3T3-A31 fibroblasts were kindly donated by Dr. Mari Cleide Sogayar (Chemistry Institute, University of São Paulo, SP, Brazil); while K562 chronic myelogenous leukemia cells were obtained from the Rio de Janeiro Cell Bank (Rio de Janeiro, RJ, Brazil). The 3T3 and K562 cells were cultured in DMEM or RPMI-1640 medium, respectively, supplemented with 10% (v/v) heat-inactivated FBS, 2 mM L-glutamine, 4.5 mM HEPES, 0.17 M sodium bicarbonate, 100 IU/mL penicillin and 100 µg/mL streptomycin in a humidified atmosphere of 5% CO_2 in air at 37 °C.

2.3. Animals

Female Swiss mice, weighing between 30 and 35 g, obtained from the Bioterium at the Federal University of Goiás (Goiânia, GO, Brazil) were used in this study. All efforts were realized to ensure the welfare of mice. Parameters as loss of body weight, food/water consumption and changes in activity and behavior of the animals were daily checked as clinical conditions of animal suffering to determine when the animals must be humanely sacrificed [26]. In addition, mice were acclimatized for a week before beginning the experiments.

The animals were kept under constant environmental conditions with a light-dark (12:12 h) cycle, controlled temperature (23 ± 2 °C), water and food provided *ad libitum*. All procedures and protocols were reviewed and approved by the Research Ethics Committee of the Federal University of Goiás (UFG no. 137/2009). At the end of each experiment, the mice were previously anesthetized with xylazine (10 mg/kg) and ketamine hydrochloride (100 mg/kg) administered intraperitoneally and then euthanized by cervical dislocation [26].

2.4. General

NMR experiments were acquired at room temperature on a BrukerAvance III 500 (11.75 T) spectrometer, using a 5 mm inverse-detection probehead with z-gradient. To acquire ^{1}H and ^{13}C experiments, samples containing 20 mg of LQFM018 (**2**) in $CDCl_3$ and tetramethylsilane (TMS) as internal standard were used. 1D and 2D pulse sequences from the Bruker user library were used for all experiments. Infrared (IR) spectra were obtained on a Nicolet-55a Magna spectrometer using KBr plates. Mass spectra (MS) were obtained with a microTOF III (Brucker Daltonics Bremen, Germany). The sample preparation for MS analysis consisted of diluting 1 µg of sample in 1 mL of methanol. To perform the analysis in positive mode, 1 µl of formic acid was added to the sample. The solution obtained was directly infused at a flow rate of 3 µL/min into the ESI source. ESI(+) source conditions were as follows: nebulizer nitrogen gas temperature and pressure of 2.0 bar and 200 °C, capillary voltage of −4,5 kV, transfer capillary temperature of 200 °C; drying gas of 4 L min−1; end plate offset of

−500 V; skimmer of 35 V and collision voltage of −1.5 V. Each spectrum was acquired using 2 microscans. The resolving power (m/Δm50% 16.500,00, where Δm50% is the peak full width at half-maximum peak height). Mass spectra were acquired and processed with Data Analysis software (BruckerDaltonics, Bremen, Germany). The progress of all reactions was monitored by aluminum flexible plates for thin-layer chromatography (TLC), using a 0.25 mm layer of silica gel 760 (Merck). The compounds were revealed by UV_{254}, UV_{265} and iodine vapor.

2.5. Synthesis of LQFM018 (2)

To a 50 mL bottom flask, 1.00 mmol of 1-(4-chlorophenyl)-1H-pyrazole-4-carbaldehyde (**6**),1.00 mmol of ethyl *N*-piperazinecarboxylate (**7**), 0.5 mmol of $ZnCl_2$, 0.5 mmol, 5 mL of methanol and $NaCNBH_3$ were added. The reaction was carried out at room temperature for 2 h. The solvent was evaporated and the residue partitioned between NaOH (1N) and CH_2Cl_2. The combined organic layers were dried with Na_2SO_4 and concentrated by vacuum. Flash column was used to afford LQFM018 (**2**) as a beige solid, in 47% of yield, mp 41 °C, Rf = 0.72 (CH_2Cl_2:MeOH, 95:5).^{1}H NMR (500 MHz) $CDCl_3$/TMS (δ): 7.85 (1H, s, H5); 7.63 (1H, s, H3); 7.62 (2H, d, J = 9.0 Hz, H2′ and 6′); 7.40 (2H, d, J = 9.0 Hz, H3′ and 5′); 4.13 (2H, q, J = 7.2 Hz, H14); 3.52–3.46 (4H, s, H9 and 11); 3.49 (2H, s, H6); 2.46–2.41 (4H, m, H8 and 12); 1.25 (3H, t, J = 7.2 Hz, H15); RMN ^{13}C (125 MHz) $CDCl_3$/TMS (δ): 155.4 (C-13); 142.0 (C-3); 138.6 (C-4′); 131.9 (C-1′); 129.5 (C-3′ and 5′); 126.5 (C-5); 120.0 (C-2 and 6′); 119.7 (C-4); 61.3 (C-14); 52.5 (C-8 and 12); 52.3 (C-6); 43.5 (C-9 and 11); 14.6 (C-15); I.R.$_{max}$ (KBr) cm^{-1}: 3107 (ν C—H); 2983 (ν C—H); 1690 (ν C═O);1501 (ν C═C); 1092 (ν C—Cl); MS: $[M + H]^+$ *m/z* of 349.1392; $[M + Na]^+$ *m/z* of 371.1197; purity > 98% (Supplementary Figs. 1–6).

2.6. Preparation of LQFM018 (2)-containing formulation

For the *in vitro* assays, an emulsion containing LQFM018 (**2**) was prepared as follows to allow dissolution in water: 5 mg of LQFM018 (**2**) were diluted in 200 μL ethanol, to which 5 mg phosphatidylcholine and 800 μL sodium taurodeoxycholate hydrate solution (1.25 mg/mL) were added in water. For the *in vivo* assay, LQFM018 (**2**) was dissolved in sunflower oil for administration to mice.

2.7. Binding assays

Binding assays were carried out as described elsewhere [27]. In brief, membrane preparations of cells transfected with human receptors (Chemiscreen, Millipore) were used with 0.1 nM [^{3}H]-YM-09151-2 as radioligand for the dopamine D_4 receptors. For binding to the D_2-like receptors, striatal membranes from rat brain were used with the same radioligand. For serotonin 5-HT_{1A} and 5-HT_{2A} receptors, hippocampal and cortical membranes from rat brain were used with 1 nM [^{3}H]-8-OH-DPAT and 1 nM [^{3}H]-ketanserin, respectively.

2.8. Cytotoxicity assays

Trypan blue exclusion, MTT reduction and lactate dehydrogenase (LDH) release assays were carried out to evalute the cytotoxicity of LQFM018 (**2**). In brief, K562 cells (1 × 10^6 cells/mL) were seeded into 96-well flat plates in RPMI medium supplemented with 10% (v/v) FBS and incubated with or without eight concentrations of LQFM018 (**2**) (10–1430 μM) in sextuplicate for 24, 48 or 72 h.

After the treatment, an aliquot of cell suspension was mixed with trypan blue solution (0.2% in phosphate buffered saline, PBS) (1:10) and the viability of the cells was estimated using a hemocytometer (Reichert, USA). Those cells which incorporated the dye and turned blue were quantified as dead [28].

For the MTT assay [29], 10 μL/well MTT (5 mg/mL) were added and plate incubated for additional 4 h. Posteriorly, cells were centrifuged at 800 rpm for 10 min, the supernatant removed and 100 μL of DMSO added in each well to solubilize the formed formazan. Absorbance was measured at 545 nm using a spectrophotometer (Stat Fax 2100, Awareness Technology, Dusseldorf, Germany). The IC_{25} or IC_{50} values (concentration that inhibited cell growth by 25 or 50% in comparison to untreated group) obtained in the MTT assay over 24 h of treatment was used for subsequent studies.

The levels of LDH released by K562 cells after the treatment with and without LQFM018 (**2**) for 24 h were estimated using the Lactate Dehydrogenase Activity Assay kit (Sigma-Aldrich) in accordance with the manufacturer's instructions.

2.9. Cell morphology examination

After 24 h of treatment with LQFM018 (**2**) (427 μM), cells (1 × 10^5 cells/mL) were placed on glass slides and stained by May-Grünwald-Giemsa dye [76] at room temperature for 10 min. After staining, the slides were examined by light microscopy (AxioZeiss, Zeiss, Germany) and images were analyzed at 400× magnification. In addition, nuclear changes were assessed using the DNA binding dye Hoechst 33342 as follows: cells were fixed in a solution of acetic acid and methanol (1:3) for 10 min and 100 μL of Hoechst 33342 dye (10 μg/mL) were added and left to incubate for 10 min. Posteriorly, cells were washed in deionized water and the slides were analyzed by fluorescence microscopy (DMI 4000 B Leica Microsystems, Bannockburn, IL, USA) using a 400× magnification and LAS-AF software, filter A4.

2.10. Cell cycle analysis

K562 cells (1 × 10^6 cells/mL) treated with or without LQFM018 (**2**) (427 μM) were washed twice with ice-cold PBS at 1500 rpm for 10 min and fixed with 1 mL ice-cold 70% ethanol at 4 °C. After 24 h, cells were washed in PBS and incubated with 1 mL PBS solution containing RNAse (200 μg/mL) and PI (50 μg/mL) at room temperature in the dark for 2 h. The red PI fluorescence was excited by a wavelength of 488 nm and detected at 620–700 nm filter using a flow cytometer (BD FACSCanto II, BD Biosciences, San Jose, CA, USA) recording 10,000 events for each analysis in duplicate.

2.11. Phosphatidylserine externalization

Phosphatidylserine externalization assessment was carried out using a FITC Annexin V Apoptosis Detection kit (BD Bioscience), in accordance with manufacturer's instructions. Briefly, K562 cells (1 × 10^6 cells/mL) were incubated with and without LQFM018 (**2**) (427 μM) for 24 h and washed with ice-cold PBS at 1500 rpm for 10 min. After that, the cells were rewashed in 100 μL of binding buffer (10 mmol/L HEPES/NaOH, 140 mmol/L NaCl, 2.5 mmol/L $CaCl_2$) at 1500 rpm for 10 min. Then 5 μL of FITC-conjugated Annexin V (A) were added and the cells incubated at room temperature for 15 min. They were then washed with binding buffer, and 200 μL of binding buffer containing PI solution (5 μg/mL) were added. The stained cells were analyzed by flow cytometer to determine four cell populations: necrotic (A−/PI+), early apoptotic (A+/PI−), late apoptotic (A+/PI+) and viable (A−/PI−) cells.

2.12. Evaluation of mitochondrial membrane potential (ΔΨm) and reactive oxygen species (ROS) generation

After treatment with LQFM018 (**2**) (427 μM) for 6, 12 or 24 h, K562 cells (1 × 10^6 cells/mL) were washed with 1 mL PBS at 1500 rpm for 10 min. The supernatant was then removed and 1 mL of rhodamine 123 (1 μg/mL) or DCFH-DA (10 μM) solution were added to evaluate loss of ΔΨm and ROS production, respectively. After incubation of 1 h, cells

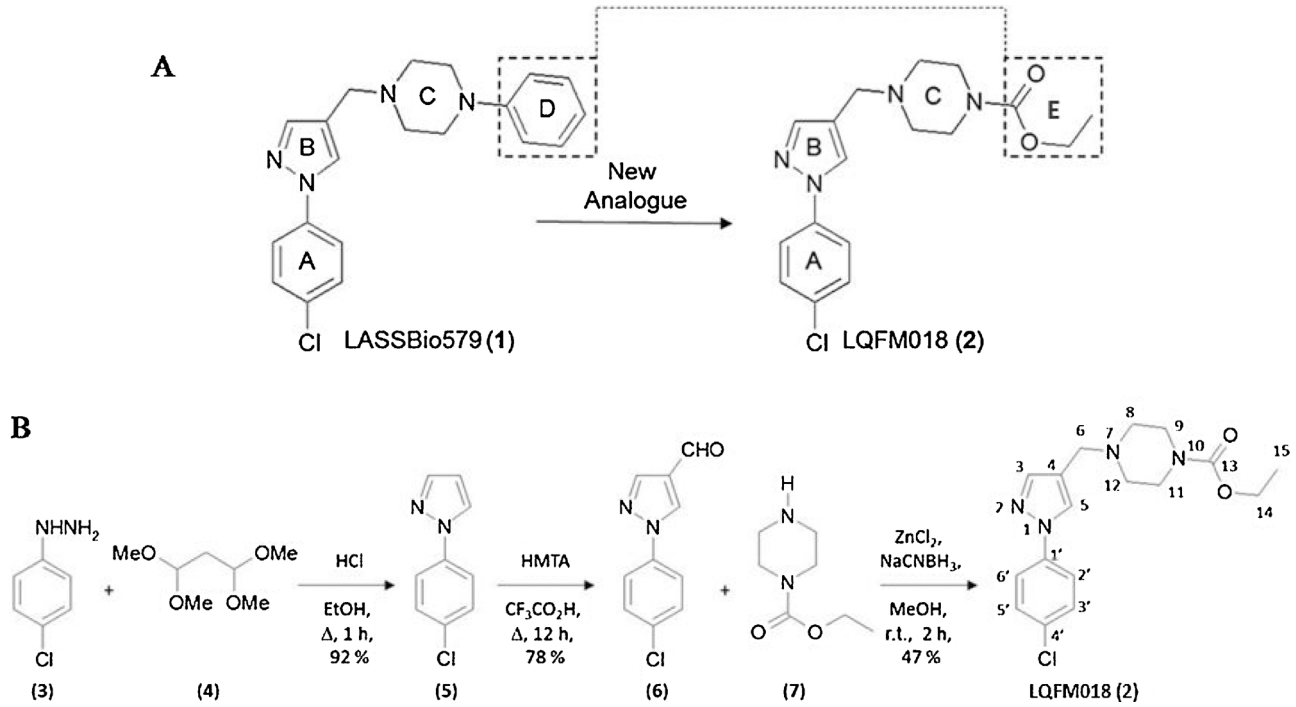

Fig. 1. Design (A) and synthetic route (B) of the LQFM018 (**2**) from the LASSBio 579 (**1**).

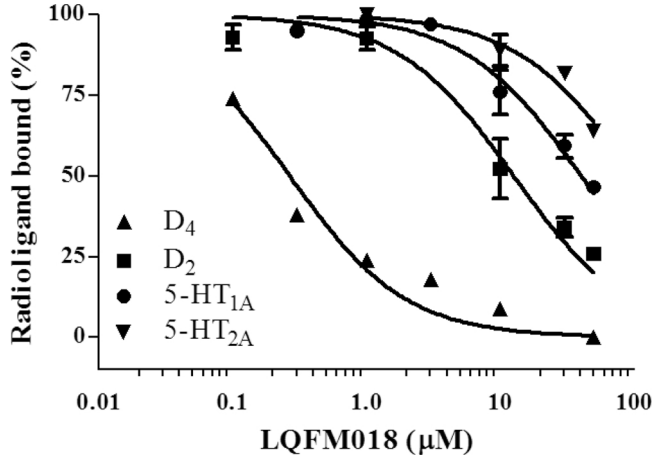

Fig. 2. Competition curves for the binding of LQFM018 (**2**) to the dopamine (D_2 and D_4) and serotonin (5-HT_{1A} and 5-HT_{2A}) receptors. The mean data of three independent experiments were fitted assuming a single population of binding sites.

Table 1
K_i values (μM) for LQFM018 (**2**) at dopamine (D_2 and D_4) and serotonin (5-HT_{1A} and 5-HT_{2A}) receptors.

Compound	D_2	D_4	5-HT_{1A}	5-HT_{2A}
Clozapine[a]	0.14	0.060	0.26	0.021
LASSBio579[a]	0.39	0.18	0.22	6.91
LQFM018	10.2	0.26	≈ 17	≈ 73

≈ low precision (about or less than 50% inhibition at 50 μM, the higher concentration tested due to solubility limitation).

K_i values were calculated by the Cheng-Prusoff equation using IC_{50} values estimated from Fig. 2.

K_d values estimated in saturation experiments: 0.42, 2.74, 0.70 and 2.69 nM for D_2, D_4, 5-HT_{1A} and 5-HT_{2A} receptors, respectively.

[a] From Pompeu et al. [27].

were washed, resuspended in 400 μL of PBS and evaluated by flow cytometer.

2.13. Analysis of cytochrome c release and expression of TNF-R1

K562 cells (1×10^6 cells/mL) were washed twice in ice-cold PBS-BSA soon after the treatment with and without LQFM018 (**2**) (427 μM) for 24 h. After that, 5 μL anti-TNF-R1 or anti-cytochrome c antibodies were added and incubated at room temperature protected from light for 20 min. Cells were then washed twice with PBS and resuspended with 400 μL of PBS for analysis by flow cytometer.

2.14. Determination of caspase-3 and -8 activities

K562 cells (1×10^6 cells/mL) were treated with and without LQFM018 (**2**) (427 μM) for 24 h and cell lysate was used to determine caspase activity using a Caspase-3 Colorimetric Assay kit (Sigma-Aldrich), according to the manufacturer's guidelines. Caspase-8 activity assessment was carried out using the CaspaTag Caspase *In Situ* Assay Fluorescein kit (Millipore™) following the manufacturer's instructions.

2.15. Quantitative RT-PCR

The transcriptional profiles of caspase-3 and-8, factor nuclear kappa B (NF-κB) and cylindromatosis (CYLD) were analyzed after treatment of K562 cells with LQFM018 (**2**) (213 μM). Total RNA from K562 cells was obtained using the RNeasy mini kit (Qiagen), following the manufacturer's instructions. The concentration and purity of the isolated RNA were determined by measuring the optical density at 260 and 280 nm using NanoDrop 8000 spectrophotometer (Thermo Fisher Scientific, Waltham, MA, USA). RNA integrity was verified by electrophoresis through 1.5% agarose gel stained with ethidium bromide. QuantiTect Reverse Transcription Kit (Qiagen) was used for cDNA synthesis with 1 μg of RNA, in accordance with the manufacturer's instructions. Real-time PCR was performed with 2.5 μL cDNA diluted 1/2 and 300 nM of primers using Rotor-Gene SYBR Green PCR kit (Qiagen). DNase I treatment for gDNA digestion was done with an RNeasy mini and QuantiTect Reverse Transcription kits (Qiagen) following the manufacturers' instructions. PCR specificity was determined using both

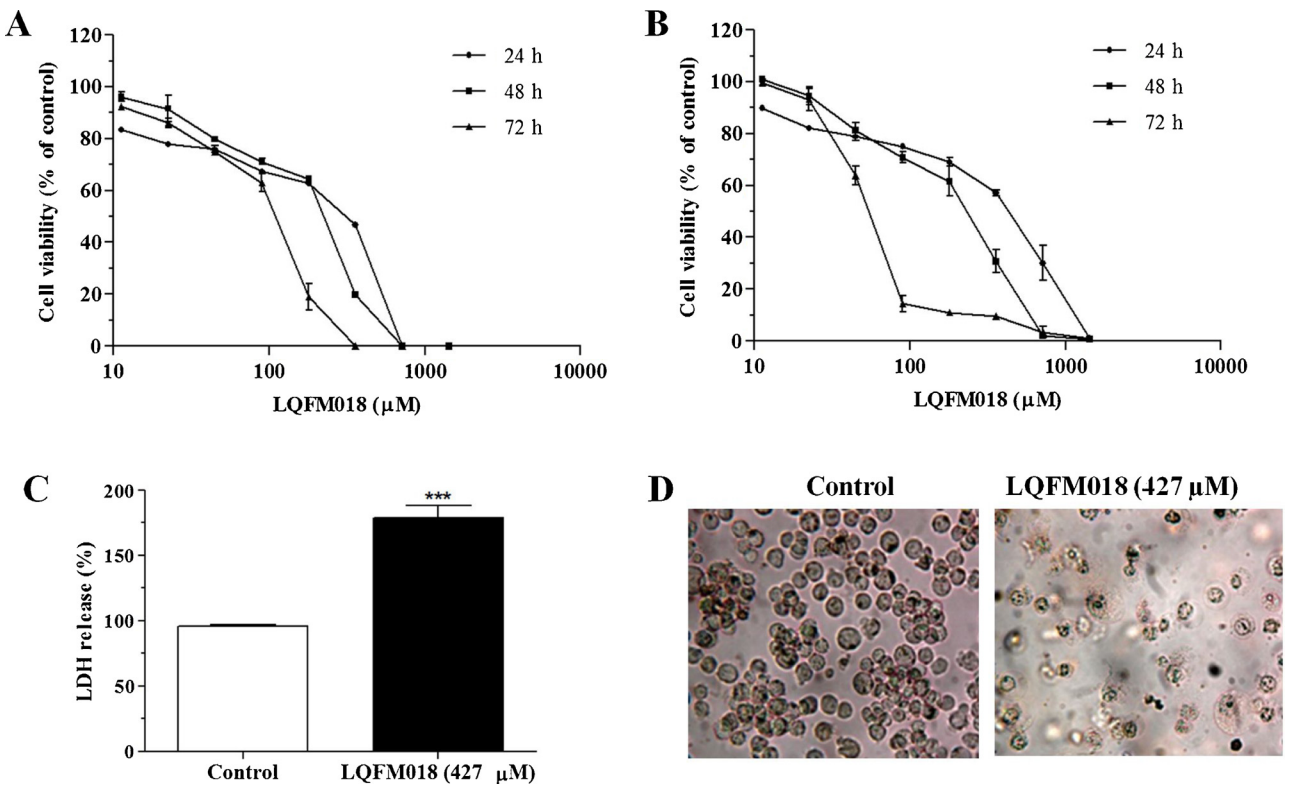

Fig. 3. Cytotoxicity evaluation of LQFM018 (**2**) in K562 leukemic cells. Cells were treated with different concentrations of LQFM018 (**2**) (10–1430 μM) for 24, 48 or 72 h. After that, cytotoxicity evaluation was carried out using trypan blue exclusion (A) and MTT reduction (B) assays. LDH release assay (C) was also conducted in K562 cells treated with LQFM018 (**2**) (427 μM) for 24 h. (D) Aspect of K562 cells treated with or without of LQFM018 (**2**) (427 μM) for 24 h. The images were taken using a 200x objective. ($^{***}p < 0.001$ *vs.* control). Each point represents mean ± SD of three independent experiments.

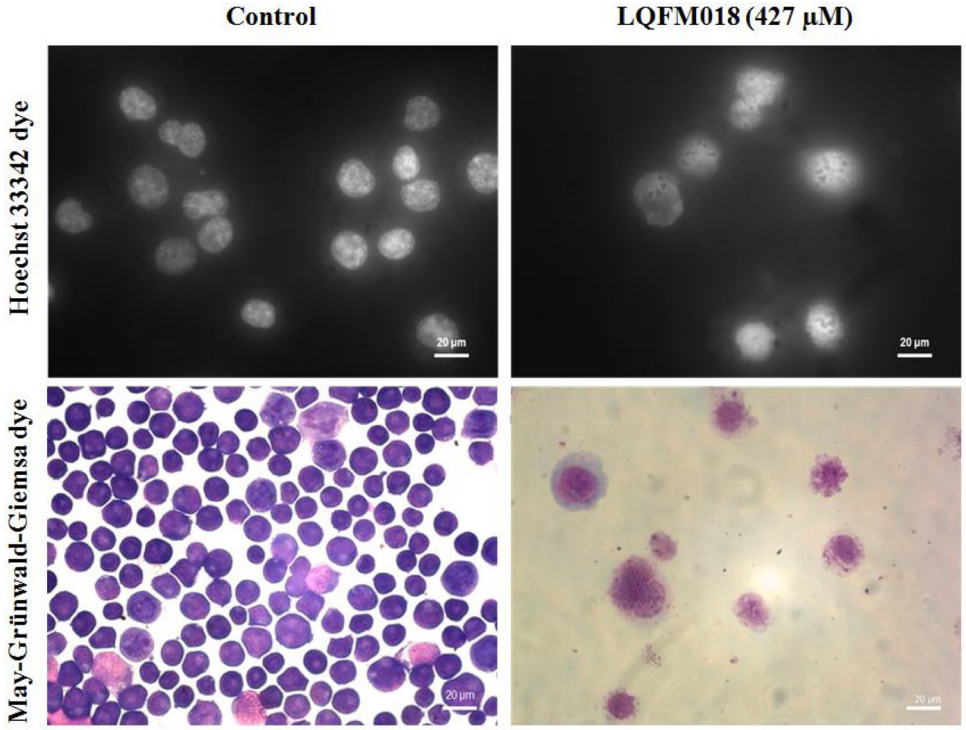

Fig. 4. Morphological analysis of K562 leukemic cells treated with or without LQFM018 (**2**) (427 μM) for 24 h using DNA binding dye Hoechst 33342 and May-Grünwald-Giemsa dyes (magnification ×400).

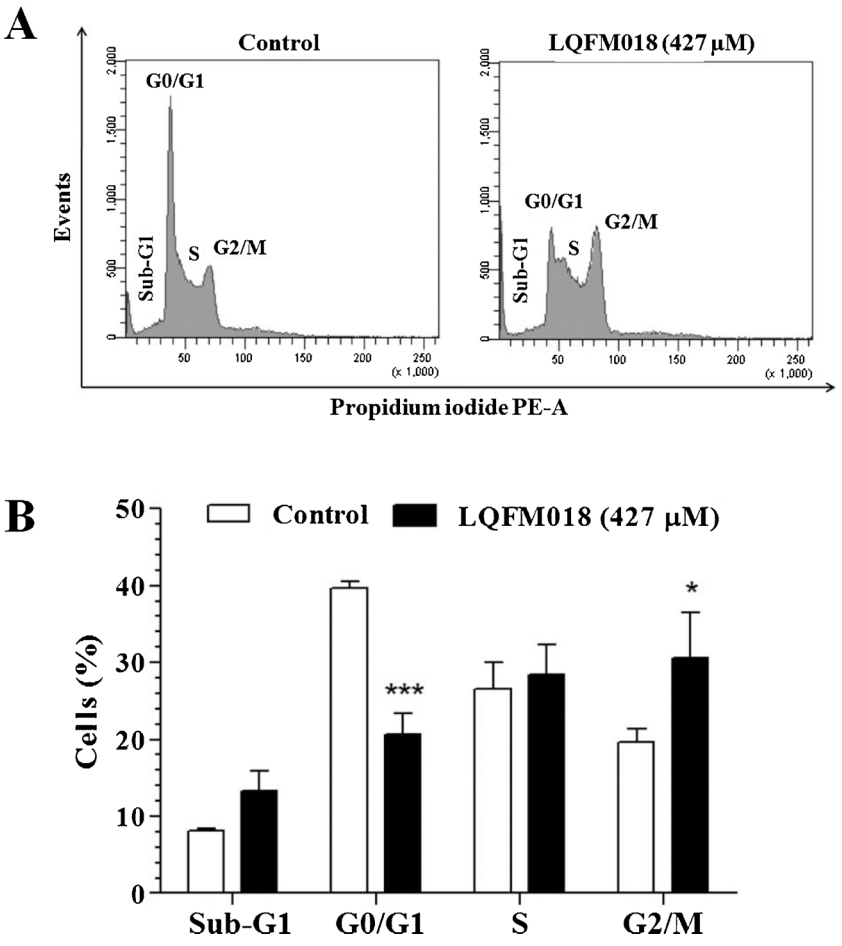

Fig. 5. Cell cycle analysis of K562 leukemic cells treated without or with LQFM018 (**2**) (427 µM) for 24 h. (A) Representative histograms of cell cycle of untreated and treated K562 cells. (B) Percentage of cells in sub-G1, G0/G1, S and G2/M phases. Each bar represents mean ± SD of two independent experiments. ($^{*}p < 0.05$ and $^{***}p < 0.0001$ *vs.* control).

a melting curve analysis and gel electrophoresis. The sequences of primers used were described elsewhere: CYLD [30], caspase-3 and caspase-8 [31], NF-κB [32] and beta-2-microglobulin (B2M) [33]. The following PCR conditions were used: 95 °C for 5 min followed by 40 cycles of 5 s at 95 °C and 10 s at 60 °C using Rotor-Gene Q (Qiagen, Hilden, Germany). The endogenous gene used for normalization was B2M. The relative expression was calculated using the REST 2009 method [34]. The results were obtained through three independent experiments in duplicate.

2.16. Toxicity studies

2.16.1. 3D colony forming unit-granulocyte/macrophage (CFU-GM) assay

The analysis of potential myelotoxicity of LQFM018 (**2**) was performed by 3D clonogenic assay of CFU-GM, proposed by [35] and modified by Mota et al. [28]. Briefly, bone marrow cells were collected from a mouse, transferred to a sterile tube containing RPMI medium and washed at 1500 rpm for 10 min. After that 1×10^5 cells/mL were seeded in Petri dishes (35 × 10 mm), maintained in 2 mL of 2× DMEM containing 20% (v/v) FBS, 50% (v/v) agar (0.6%, p/v), GM-CSF (0.5 ng/mL) with or without eight different concentrations of LQFM018 (**2**) (0.006–0.716 mM). The dishes were incubated for 7 days in a humidified atmosphere of 5% CO_2 in air at 37 °C. After incubation, the colony forming units were scored at 35× magnification using a dissection microscope (Leica, Wetzlar, Germany).

2.16.2. Neutral red uptake (NRU) assay

This assay was conducted according to the NICEATM standard protocol [36]. In brief, 3T3 fibroblasts (3×10^4 cells/mL) were seeded into a 96-well flat plate in DMEM supplemented with 10% (v/v) FBS and incubated for 24 h. The medium was removed and eight different concentrations of LQFM018 (**2**) (11–1433 µM), diluted in complete medium, were added in each well in sextuplicate. After 48 h of incubation, the treatment medium was removed and all wells received a solution containing 250 µL of neutral red dye (0.25 mg/mL) diluted in medium (DMEM + 5% FBS) followed incubation of 3 h. The NR medium was discarded and cells were washed once with PBS (250 µL/well). The supernatant was removed and 100 µL/well of NR desorb (1% acetic acid, 50% ethanol and 49% deionized water) solution were added. The plate was shaken on a microplate shaker for 20 min to extract NR from the cells forming a homogeneous solution. The absorption was measured at 545 nm in a spectrophotometer. The estimated LD_{50} (dose that causes death in 50% of animals) was estimated based on the equation previously established [37]: Log (LD_{50}) = 0.545 × log (IC_{50}) + 0.757.

2.16.3. Analysis of acute oral systemic toxicity

Considering that animal experimentation still remains essential to meet regulatory requirements, the *in vivo* analysis in this study were performed focused on animal welfare. The experimental design considered the minimum number of animals without reducing the scientific integrity of data generated [38]. Thus, *in vivo* confirmation of the estimated LD_{50} of LQFM018 (**2**), established as described in item 2.16.2, was conducted according to the OECD Test Guideline No. 423 - Acute Toxic Class Method [38]. Based on scientific progress, this validated test uses a reduced number of animals to judge acute toxicity of a substance and classify it according to the United Nations Globally Harmonized System of Classification and Labelling of Chemicals (UN

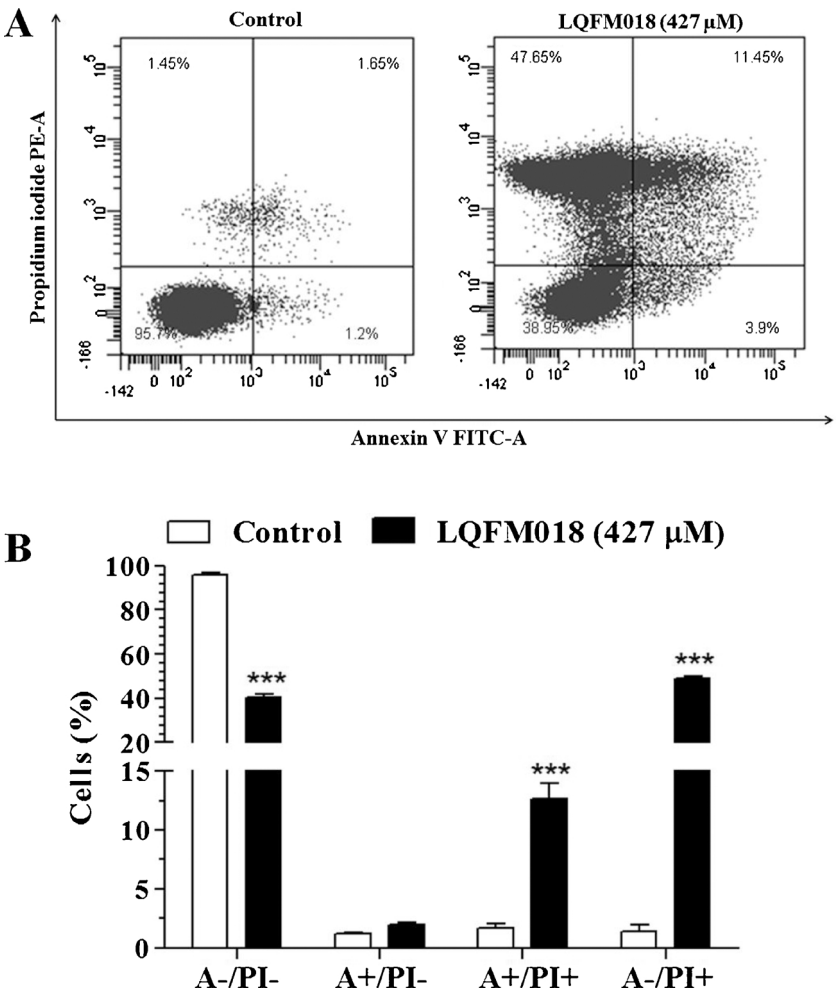

Fig. 6. Evaluation of phosphatidylserine externalization in K562 leukemic cells treated with or without LQFM018 (**2**) (427 µM) for 24 h using Annexin V (A)/propidium iodide (PI) double staining assay. (A) Representative histograms of untreated and treated K562 cells showing the following populations: viable (A−/PI−, left lower quadrant), early apoptotic (A+/PI−, right lower quadrant), late apoptotic (A+/PI+, right upper quadrant) and necrotic (A−/PI+, upper left quadrant) cells. (B) Percentage of viable, apoptotic and necrotic cells in untreated and treated cells. Each bar represents mean ± SD of two independent experiments. (***$p < 0.0001$ *vs.* control).

GHS). In brief, two groups of three female Swiss mice were treated orally (by gavage) with a single dose (0.2 mL/mice) of 500 and 2000 mg/Kg of LQFM018 (**2**). The animals were observed for the first 10 min, 30 min, 1 h, 2 h, 4 h, 6 h, 12 h and 24 h and daily until the 14th day after treatment. A Hippocratic screening was performed to investigate the following signs: vocal tremor, irritability, touch response, response to the tightening of tail, righting reflex, body tone, tremors, convulsions, straub, piloerection, cyanosis, salivation and death. The intensities of these events were tabulated from 0 to 4 (absent, rare, little, moderate and intense, respectively). Behavioral changes were recorded in a protocol according to Malone [39]. As recommended, the safety of the estimated LD_{50} was subsequently confirmed in another three animals. The abdominal cavity was opened to check for possible macroscopic alterations.

2.17. Statistical analysis

For flow cytometer analysis, 10,000 events were collected per sample of each assay using a FACSCanto II flow cytometer and FACSDiva software version 6.0 (BD Biosciences, San Jose, CA, USA). Statistical analysis was performed by two-way ANOVA followed by Bonferroni post-test or Student's *t*-test using GraphPad Prism version 5.0 software for Windows (San Diego, CA, USA). The data are expressed as mean ± standard deviation (SD) of two or three independent assays. Statistical significance was established as $p < 0.05$.

3. Results

3.1. Synthesis of LQFM018 (2)

LQFM018 (**2**) was designed as a new analogue from LASSBio579 (**1**), a compound obtained from the atypical antipsychotic clozapine. As can be seen in Fig. 1A, the subunits A, B and C present in LASSBio579 (**1**) were preserved, whereas the phenyl subunit (D) was changed by ethyl carbamate (E) to increase the metabolic stability of LQFM018 (**2**). Furthermore, LQFM018 (**2**) presents the pharmacokinetic filters preconized by Lipinsky. As shown in Fig. 1B, its synthetic route began by synthesis of 1-(4-chlorophenyl)-1*H*-pyrazole (**5**) compound using the classical method described by Finar and Godfrey [77], in 92% of yield. On the other hand, compound 1-(4-chlorophenyl)-1H-pyrazole-4-carbaldehyde (**6**) was produced in 78% of yield through chemospecific and regiospecific formulation of 1-(4-chlorophenyl)-1H-pyrazole (**5**), which was performed under Duff's conditions. The last step was carried out through reductive amination conditions in 47% of yield. After three synthetic steps, LQFM018 (**2**) was obtained in 33% of global yield.

3.2. Binding profile to aminergic receptors

It was determined the affinity of LQFM018 (**2**) for aminergic receptors that are involved in the therapeutic effect of atypical antipsychotics. Fig. 2 and Table 1 show that LQFM018 (**2**) has moderate

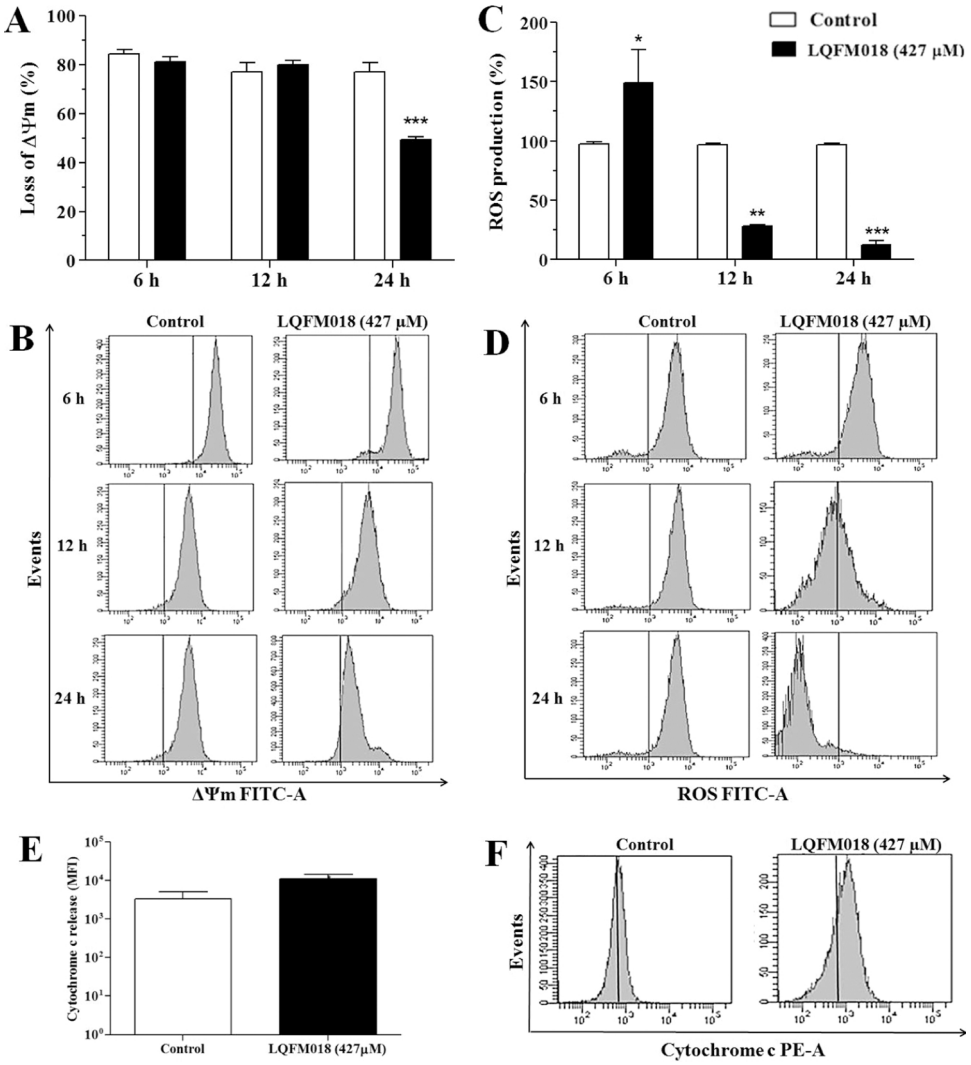

Fig. 7. Effects of LQFM018 (**2**) on the ΔΨm, ROS generation and cytochrome c release in K562 leukemic cells. Cells were treated with or without LQFM018 (**2**) (427 μM) for 6, 12 or 24 h. After that, ΔΨm (A and B) and ROS generation (C and D) assessments were carried out using rhodamine 123 and DCFH-DA staining, respectively. (E and F) Cytochrome c release analysis in control and cells treated with LQFM018 (**2**) (427 μM) for 24 h. Flow cytometric histograms (B, D and F) are representative of each assay. Each bar represents mean ± SD of two independent experiments. ($^{*}p < 0.05$, $^{**}p < 0.001$ and $^{***}p < 0.0001$ *vs.* control).

affinity for the dopamine D_4 receptor (K_i = 0.26 μM), like LASSBio579 and clozapine, but much less affinity for the dopamine D_2, serotonin 5-HT_{1A} and 5-HT_{2A} receptors.

3.3. Cytotoxicity induced by LQFM018 (2) in K562 cells

The cytotoxicity of LQFM018 (**2**) in K562 cells was evaluated in 24, 48 and 72 h of treatment using trypan blue and MTT assays. Data showed that this compound promoted a decrease in K562 cell viability in a concentration and time-dependent manner. The IC_{50} values obtained for each exposure time were 399, 242 and 119 μM for trypan blue test (Fig. 3A) and 427, 259 and 50 μM for the MTT method (Fig. 3B). In addition, cell membrane integrity of K562 cells treated with LQFM018 (**2**) (427 μM) for 24 h was analyzed by LDH release assay. It was observed that LQFM018 (**2**) promoted an increase of 179.17% in LDH release when compared to control cells ($p < 0.0001$) (Fig. 3C). Morphological changes were also observed after treatment of K562 with LQFM018 (**2**) (Fig. 3D).

3.4. Morphological analysis of K562 cells treated with LQFM018 (2)

To further explore the morphological changes after treatment with LQFM018 (**2**) (427 μM), K562 cells were stained with Hoechst 33342 and May-Grünwald-Giemsa. Predominant necrotic morphologies were observed, including gain in cell volume (oncosis), plasma membrane rupture and subsequent loss of intracellular content (Fig. 4).

3.5. Effects of LQFM018 (2) on cell cycle of K562 cells

Fig. 5A shows a representative cell cycle of K562 cells treated with or not LQFM018 (**2**) (427 μM) for 24 h. It was observed that LQFM018 (**2**) promoted a significant decrease of 20.60% in the proportion of cells in the G0/G1 phase in comparison to control ($p < 0.0001$). In addition, it triggered a significant increase of 30.63% ($p < 0.05$) in G2/M phase, which indicates a tendency of the cells to arrest in this phase of the cell cycle. No change was observed in the S phase. In relation to sub-G1 phase, characterized by DNA fragmentation due to apoptosis, it was observed an increase of 13.30%, although not statistically significant (Fig. 5B).

3.6. Evaluation of phosphatidylserine exposure induced by LQFM018 (2) in K562 cells

Assessment of phosphatidylserine exposure induced by treatment of

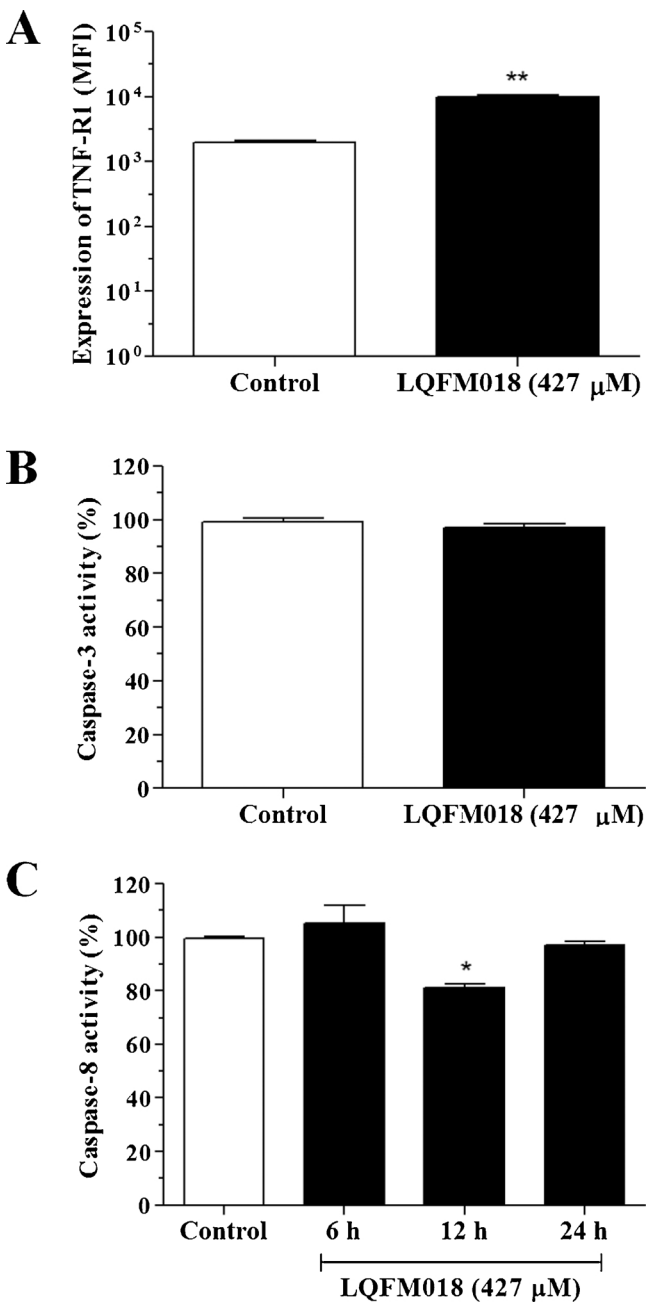

Fig. 8. Effects of LQFM018 (**2**) on TNF-R1 expression and caspase-3 and -8 activities in K562 leukemic cells. Cells were treated with or without LQFM018 (**2**) (427 μM) for 24 h and expression of TNF-R1 (A) and caspase-3 activity (B) were carried out. (C) Caspase-8 activity of cells treated with or without LQFM018 (**2**) (427 μM) for 6, 12 or 24 h. Each bar represents mean ± SD of two independent experiments. ($^{*}p < 0.05$ and $^{**}p < 0.001$ *vs.* control).

LQFM018 (**2**) (427 μM) for 24 h in K562 cells was evaluated by A/PI double staining flow cytometric assay. As show in Fig. 6A and B, LQFM018 (**2**) promoted a significant decrease of 40.50% in cell viability (A−/PI−) ($p < 0.001$) in contrast to the control cells. Moreover, the percentage of early (A+/PI−) and late (A+/PI+) apoptotic cells were 1.95 and 11.40% ($p < 0.0001$), respectively. Furthermore, this compound significantly triggered necrosis (A−/PI+) in 47.60% of the K562 cells ($p < 0.0001$) in relation to the control.

3.7. Effects of LQFM018 (2) on the ΔΨm, ROS generation and cytochrome c release in K562 cells

The effects of LQFM018 (**2**) on ΔΨm and ROS generation using K562 cells were assessed by rhodamine 123 and DCFH-DA staining, respectively. It was verified that the treatment of the cells with LQFM018 (**2**) (427 μM) for 6 and 12 h did not promote changes in ΔΨm. On the other hand, the treatment for 24 h triggered a significant loss of ΔΨm ($p < 0.0001$), in comparison to control (Fig. 7A and B). LQFM018 (**2**) also promoted a significant increase in ROS production after 6 h of treatment ($p < 0.05$), whereas the ROS levels were statistically reduced after 12 h ($p < 0.001$) and 24 h ($p < 0.0001$) (Fig. 7C and D). No significant accumulation of cytosolic cytochrome c was verified in treated cells with LQFM018 (**2**) for 24 h (Fig. 7E and F).

3.8. Effects of LQFM018 (2) on TNF-R1 expression and caspase-3 and -8 activities in K562 cells

The treatment of K562 cells with LQFM018 (**2**) (427 μM) for 24 h significantly increased the expression of TNF-R1 protein ($p < 0.001$) (Fig. 8A). In addition, no statistical difference was verified in caspase-3 activity (Fig. 8B), whereas caspase-8 activation failed, especially at 12 h after treatment ($p < 0.05$) (Fig. 8C).

3.9. Effects of LQFM018 (2) on mRNA levels of caspase-3 and -8, NF-κB and CYLD in K562 cells

Quantitative analysis of mRNA levels of caspase-3 and -8, NF-κB and CYLD in K562 cells treated with LQFM018 (**2**) (213 μM) were carried out using RT-PCR. As shown in Fig. 9, only the mRNA levels of CYLD were increased after treatment with LQFM018 (**2**).

3.10. Toxicity evaluation of LQFM018 (2)

3.10.1. Effects of LQFM018 (2) in murine hematopoietic precursors

The assessment of potential myelotoxicity of LQFM018 (**2**) was carried out in murine hematopoietic precursors using 3D CFU-GM assay. As shown in Fig. 10, LQFM018 (**2**) did not significantly decrease the CFU-GM number at concentrations of 6–22 μM, when compared to the control. On the other hand, it promoted a concentration-dependent reduction of these progenitor cells ($p < 0.05$) at higher concentrations (45-716 μM), which suggests that LFQM018 could have an immunosuppressive effect at the concentration studied. The IC_{50} value obtained was 300 μM.

3.10.2. Effect of LQFM018 (2) in 3T3 cells

The NRU assay in 3T3 fibroblasts revealed that the three highest concentrations of the LQFM018 (**2**) (89, 179 and 358 μM) promoted a concentration-dependent reduction in 3T3 cell viability after 48 h of treatment (Fig. 11). The IC_{50} obtained was 76.5 μM. This value was used to estimate the LD_{50}, which resulted in a dose of 500 mg/kg. Thus, the compound was classified in category 4 ($300 < LD_{50} < 2000$ mg/kg), according to the United Nations Globally Harmonized System of Classification and Labelling of Chemicals (UN GHS).

3.10.3. Evaluation of acute oral systemic toxicity in mice

In vivo confirmation of the LD_{50} estimated by the NRU assay was carried out according to the OECD Test Guideline No. 423 [38]. A single dose of 500 mg/kg LQFM018 (**2**) was administered to mice (n = 3) and it was observed no death and toxic effects during the study period (14 days of observation). Thus, other animals (n = 3) were treated with a higher dose of 2000 mg/kg LQFM018 (**2**). After treatment, some changes were observed according to the Hippocratic screening (Table 2). In addition, this dose caused the death of one animal. The necropsy showed no macroscopic alterations in the animals. Thus, LQFM018 (**2**) showed low toxicity *in vivo*, since the LD_{50} was classified

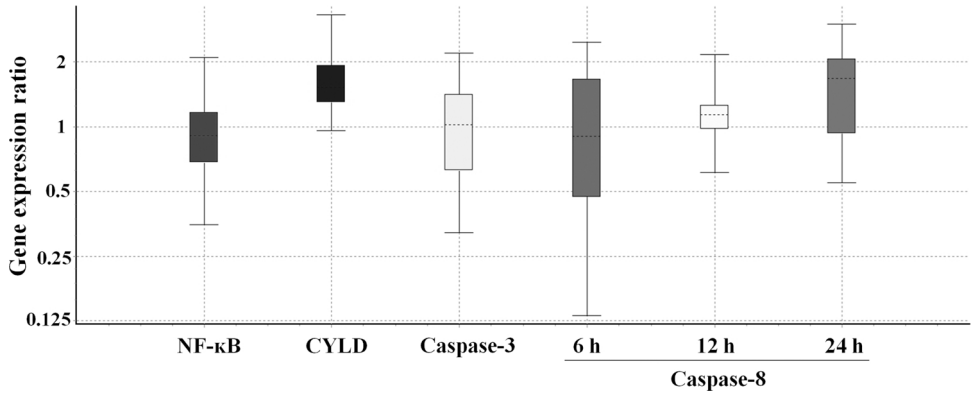

Fig. 9. Effects of LQFM018 (**2**) (213 μM) on mRNA levels of caspase-3 and -8, NF-κB and CYLD in K562 leukemic cells. The normalize gene was B2M. The relative expression was calculated using the REST 2009 method [29]. Each bar represents mean ± SD of three independent experiments.

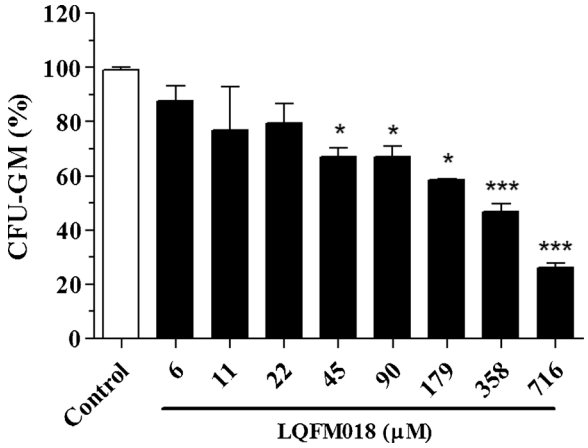

Fig. 10. Effects of LQFM018 (**2**) in murine hematopoietic precursors. Bone marrow cells were collected from a mouse and treated with or without eight different concentrations of LQFM018 (**2**) (6–716 μM) for 7 days. After incubation, colony forming units-granulocyte/macrophage (CFU-GM) were scored. Each bar represents mean ± SD of three independent experiments ($^{*}p < 0.05$ and $^{***}p < 0.0001$ *vs.* control).

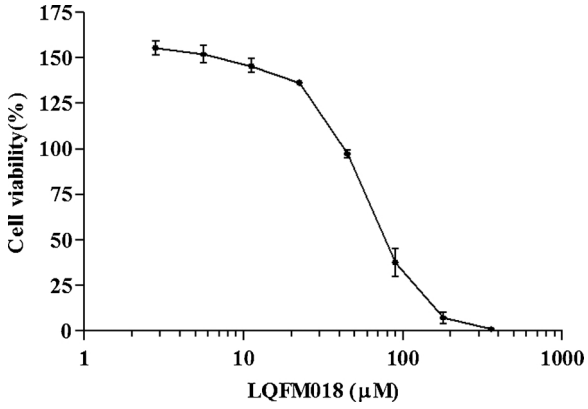

Fig. 11. Cytotoxicity of LQFM018 (**2**) in 3T3 fibroblasts. Cells were treated with or without different concentrations of LQFM018 (**2**) (11–1433 μM) for 48 h and the cell viability evaluated using neutral red uptake (NRU) assay. Each point represents mean ± SD of three independent experiments.

as UN GHS category 5 (LD_{50} > 2000–5000 mg/Kg), in agreement with OECD test guideline No. 423.

4. Discussion

As the resistance of cancer cells to apoptosis triggered by conventional anticancer therapy is a major obstacle, new agents that promote necroptosis represent a promising strategy for enhancing tumor cell sensitivity and thus to overcome neoplastic self-renewal [40,41]. In this sense, it was developed here a new piperazine-containing compound LQFM018 (**2**), which triggered cytotoxicity associated with cell cycle arrest at the G2/M stage in K562 cells with probable involvement of necroptosis pathways in the cell death process as well as possible role in dopamine D_4 receptor binding.

Table 2
Clinical signs found in mice (n = 3) treated with a single oral dose of 2000 mg/kg of LQFM018 (**2**).

Animal No.	Clinical signs[a]												
	A	B	C	D	E	F	G	H	I	J	K	L	M
1	0	0	4	4	4	4	0	0	0	0	0	0	0
2	0	0	4	4	4	4	0	0	0	0	0	0	0
3	0	0	0	0	4	4	0	0	0	0	0	3	4

[a] Abbreviations: A - vocal tremor; B - Irritability; C - touch response; D - response to tail clamp; E - righting reflex; F - forces to grab; G - tremors; H - seizures; I - straub; J - piloerection; K - cyanosis; L - salivation; M - death. The numbers represent the following: 0 - absent; 1 - rare; 2 - little; 3 - moderate; 4 - intense.

In our first evaluation, it was verified that LQFM018 (**2**) has a moderate affinity for the D_4 receptor, differently from clozapine and LASSBio579, which bind with different affinities to dopamine (D_2 and D_4) and serotonin (5-HT_{1A} and 5-HT_{2A}) receptors. This finding suggests that the D_4 receptor could play a role in the necroptosis triggered by LQFM018 (**2**). Dopamine, as well as drugs that bind to dopamine receptors, seems to play an important role against cancer cells. Different studies have shown that dopamine or its analogs have demonstrated antitumoral activities against HL60 promyelocytic leukemia [42], L1210 and P388 lymphocytic leukemia [44], K562 chronic myelogenous leukemia [43] and B16 melanoma [44] cells. In addition, clozapine has demonstrated immunomodulatory [45] and *in vitro* and *in vivo* antitumoral effects [46]. Aripiprazole, an antipsychotic drug with partial dopamine agonist activity, has also showed anticancer effects through inhibition of cancer stem cells as well as sensitizing them to chemotherapeutic agents [47].

Corroborating this, LQFM018 (**2**) triggered the following events characteristic of necroptosis in K562 cells: mitochondrial impairment through loss of ΔΨm associated with increase of ROS production, increase of expression of TNF-R1 protein and mRNA levels of CYLD, with no involvement in increased of cytosolic cytochrome c, caspase-3 and -8 activation and NF-κB. In agreement with these data, necroptosis pathways have been described *via* death receptors (*e.g.* TNF-R1 and FAS) associated with independent of the activation of caspase as well as RIPK3 and mixed lineage kinase domain-like (MLKL) activation [14,48,49]. One of the most extensively investigated models of necroptosis is that induced by the TNF-R1/tumor necrosis factor-α (TNFα)

receptor ligand system [50]. Moreover, caspase inhibition, especially caspase-8, has been implicated as a negative regulator of programmed necrosis through cleavage of RIPK and CYLD [51–53], as demonstrated here.

TNF-R1 activation through TNFα can drive cells to diverse fates. TNF-R1-mediated signaling can lead to cell survival, apoptosis or necroptosis *via* different complex formations [51,54]. After TNF-R1 activation, the TNF receptor-associated death domain (TRADD) and RIPK1 are recruited to form TRADD- and RIPK1-dependent complex I [55]. According to signalization, complex I can trigger apoptosis *via* canonical (TRADD-dependent complex IIa) and non-canonical (RIPK1-dependent complex IIb/ripoptosome) NF-kB activation. This complex can also form another macromolecular protein complex denominated RIPK3/MLKL-dependent (necrosome), which in turn triggers regulated necrosis cell death [48].

Furthermore, LQFM018 (**2**) did not alter the levels of NF-κB mRNA in K562 cells. NF-κB transcription factor, constitutively expressed in several hematologic malignancies, is critical regulator of immunity, stress responses, apoptosis and cell differentiation [56–59]. In chronic myeloid leukemia blasts, BCR-ABL protein induces constitutive activation of NF-κB [60], which inhibits TNF-induced ROS accumulation, necrotic cell death [61] and INFγ-mediated necroptosis [62].

CYLD, a tumor suppressor and a deubiquitinating enzyme, is known to be recruited by the TNFα receptor upon its activation; it has RIP1 as a substrate that inhibits the NF-κB system, triggering necroptosis [17,63]. After treatment of K562 cells with LQFM018 (**2**), mRNA levels of CYLD showed increased, which suggests that the NF-κB abrogation could be a result of CYLD activity and that RIPK1 and RIPK3 may be involved. This data also corroborates the inhibition of caspase-8 activity after LQFM018 (**2**) treatment since caspase-8 activation failure prevented CYLD degradation, resulting in necrotic death [53].

Reports have demonstrated that mitochondrial ROS overgeneration is a key-event to promote necroptosis in L929 and mouse embryonic fibroblasts [64–66], whereas this condition seems to be not crucial in HT29 human colon carcinoma and U937 human myeloid leukaemia cells [64,67]. These data suggest that the mitochondrial dependency of necroptosis may be in cell-specific context [68]. Similar results were observed in necroptotic and apoptotic processes [69–72]. The mechanistic process is not well understood, but probably requires necrosomes trafficking to mitochondria-associated membranes *via* RIPK3-MLKL interaction [73].

As regards toxicity profile of LQFM018 (**2**), it showed *in vitro* myelotoxicity potential in bone marrow cells. Similarly, clozapine, olanzapine and quetiapine also promoted cytotoxicity in myeloid progenitors [74]. Myeloid toxicity is also considered a common adverse effect in patients receiving anticancer chemotherapy [75]. Thus, LQFM018 (**2**) seems to have a non-selective action considering hematopoietic cells. Nevertheless, it was orally well tolerated, being classified as UN GHS category 5 (LD_{50} > 2000–5000 mg/Kg). Chemicals classified under this category have been considered with relative low acute oral systemic toxicity hazard [38].

5. Conclusions

Given the above, our data suggest that piperazine compound LQFM018 (**2**) promotes cell death in K562 cells *via* necroptotic signaling probably with the involvement of dopamine D_4 receptor, mitochondrial damage, TNF-R1 and CYLD induction, in contrast to failure of caspase-3 and -8 activation and NF-κB expression. These findings open new perspectives in cancer therapy by use of necroptosis inducing agents as a strategy of reverse cancer cell chemoresistance, for instance. Although LQFM018 (**2**) showed myelotoxicity potential similarly to some conventional anticancer agents, it seems to have low acute toxicity. Additional studies are necessary to further characterize toxicological profile of LQFM018 (**2**) as well as the mechanisms involved in its anticancer effects.

Acknowledgments

The authors thank the Conselho Nacional de Desenvolvimento Científico e Tecnológico (CNPq), Financiadora de Estudos e Projetos (FINEP), Instituto Nacional de Ciência Tecnologia de Fármacos e Medicamentos (INCT-INOFAR) and Coordenação de Aperfeiçoamento de Pessoal de Nível Superior (CAPES) for funding.

Appendix A. Supplementary data

Supplementary material related to this article can be found, in the online version, at doi:https://doi.org/10.1016/j.biopha.2018.02.120.

References

[1] C.S.A. Kumar, S.B.B. Prasad, K. Vinaya, S. Chandrappa, N.R. Thimmegowda, Y.C.S. Kumar, S. Swarup, K.S. Rangappa, Synthesis and *in vitro* antiproliferative activity of novel 1-benzhydrylpiperazine derivatives against human cancer cell lines, Eur. J. Med. Chem. 44 (2009) 1223–1229.
[2] L.-H. Huang, H.-D. Xu, Z.-Y. Yang, Y.-F. Zheng, H.-M. Liu, Synthesis and anticancer activity of novel C6-piperazine substituted purine steroid–nucleosides analogues, Steroids 82 (2014) 1–6.
[3] M. Deininger, E. Buchdunger, B.J. Druker, The development of imatinib as a therapeutic agent for chronic myeloid leukemia, Blood 105 (2005) 2640–2653.
[4] C.-C. Guo, R.-B. Tong, K.-L. Li, Chloroalkyl piperazine and nitrogen mustard porphyrins: synthesis and anticancer activity, Bioorg. Med. Chem. 12 (2004) 2469–2475.
[5] M.T. Weigel, L. Dahmke, C. Schem, D.O. Bauerschlag, K. Weber, P. Niehoff, M. Bauer, A. Strauss, W. Jonat, N. Maass, C. Mundhenke, *In vitro* effects of imatinib mesylate on radiosensitivity and chemosensitivity of breast cancer cells, BMC Cancer 10 (2010) 412–412.
[6] H.M. Kantarjian, F. Giles, A. Quintás-Cardama, J. Cortes, Important therapeutic targets in chronic myelogenous leukemia, Clin. Cancer Res. 13 (2007) 1089–1097.
[7] K. Kolibaba, Molecular monitoring of response in patients with chronic myeloid leukemia, Manag. Care 22 (2013) 50–61.
[8] R. Ren, Mechanisms of BCR-ABL in the pathogenesis of chronic myelogenous leukaemia, Nat. Rev. Cancer 5 (2005) 172–183.
[9] A. Perl, M. Carroll, BCR-ABL kinase is dead; long live the CML stem cell, J. Clin. Invest. 121 (2011) 22–25.
[10] S. Soverini, S. Branford, F.E. Nicolini, M. Talpaz, M.W.N. Deininger, G. Martinelli, M.C. Müller, J.P. Radich, N.P. Shah, Implications of BCR-ABL1 kinase domain-mediated resistance in chronic myeloid leukemia, Leuk. Res. 38 (2014) 10–20.
[11] Y. Xiao, C. Jiao, Y. Lin, M. Chen, J. Zhang, J. Wang, Z. Zhang, lncRNA UCA1 contributes to imatinib resistance by acting as a ceRNA against miR-16 in chronic myeloid leukemia cells, DNA Cell Biol. 36 (2016) 18–25.
[12] F. Zhao, A. Mancuso, T.V. Bui, X. Tong, J.J. Gruber, C.R. Swider, P.V. Sanchez, J.J. Lum, N. Sayed, J.V. Melo, A.E. Perl, M. Carroll, S.W. Tuttle, C.B. Thompson, Imatinib-resistance associated with BCR-ABL upregulation is dependent on HIF-1α-induced metabolic reprogramming, Oncogene 29 (2010) 2962–2972.
[13] L. Galluzzi, I. Vitale, J.M. Abrams, E.S. Alnemri, E.H. Baehrecke, M.V. Blagosklonny, T.M. Dawson, V.L. Dawson, W.S. El-Deiry, S. Fulda, E. Gottlieb, D.R. Green, M.O. Hengartner, O. Kepp, R.A. Knight, S. Kumar, S.A. Lipton, X. Lu, F. Madeo, W. Malorni, P. Mehlen, G. Nuñez, M.E. Peter, M. Piacentini, D.C. Rubinsztein, Y. Shi, H.U. Simon, P. Vandenabeele, E. White, J. Yuan, B. Zhivotovsky, G. Melino, G. Kroemer, Molecular definitions of cell death subroutines: recommendations of the nomenclature committee on cell death 2012, Cell Death Differ. 19 (2012) 107–120.
[14] L. Galluzzi, J.M. Bravo-San Pedro, I. Vitale, S.A. Aaronson, J.M. Abrams, D. Adam, E.S. Alnemri, L. Altucci, D. Andrews, M. Annicchiarico-Petruzzelli, E.H. Baehrecke, N.G. Bazan, M.J. Bertrand, K. Bianchi, M.V. Blagosklonny, K. Blomgren, C. Borner, D.E. Bredesen, C. Brenner, M. Campanella, E. Candi, F. Cecconi, F.K. Chan, N.S. Chandel, E.H. Cheng, J.E. Chipuk, J.A. Cidlowski, A. Ciechanover, T.M. Dawson, V.L. Dawson, V. De Laurenzi, R. De Maria, K.M. Debatin, N. Di Daniele, V.M. Dixit, B.D. Dynlacht, W.S. El-Deiry, G.M. Fimia, R.A. Flavell, S. Fulda, C. Garrido, M.L. Gougeon, D.R. Green, H. Gronemeyer, G. Hajnoczky, J.M. Hardwick, M.O. Hengartner, H. Ichijo, B. Joseph, P.J. Jost, T. Kaufmann, O. Kepp, D.J. Klionsky, R.A. Knight, S. Kumar, J.J. Lemasters, B. Levine, A. Linkermann, S.A. Lipton, R.A. Lockshin, C. López-Otín, E. Lugli, F. Madeo, W. Malorni, J.C. Marine, S.J. Martin, J.C. Martinou, J.P. Medema, P. Meier, S. Melino, N. Mizushima, U. Moll, C. Muñoz-Pinedo, G. Nuñez, A. Oberst, T. Panaretakis, J.M. Penninger, M.E. Peter, M. Piacentini, P. Pinton, J.H. Prehn, H. Puthalakath, G.A. Rabinovich, K.S. Ravichandran, R. Rizzuto, C.M. Rodrigues, D.C. Rubinsztein, T. Rudel, Y. Shi, H.U. Simon, B.R. Stockwell, G. Szabadkai, S.W. Tait, H.L. Tang, N. Tavernarakis, Y. Tsujimoto, T. Vanden Berghe, P. Vandenabeele, A. Villunger, E.F. Wagner, H. Walczak, E. White, W.G. Wood, J. Yuan, Z. Zakeri, B. Zhivotovsky, G. Melino, G. Kroemer, Essential versus accessory aspects of cell death: recommendations of the NCCD 2015, Cell Death Differ. 22 (2015) 58–73.
[15] L. Galluzzi, T. Vanden Berghe, N. Vanlangenakker, S. Buettner, T. Eisenberg, P. Vandenabeele, F. Madeo, G. Kroemer, Programmed necrosis: from molecules to health and hisease, in: W.J. Kwang (Ed.), Int. Rev. Cell Mol. Biol. Academic Press,

2011, pp. 1–35.
[16] M. Pasparakis, P. Vandenabeele, Necroptosis and its role in inflammation, Nature 517 (2015) 311–320.
[17] P. Vandenabeele, L. Galluzzi, T.V. Berghe, G. Kroemer, Molecular mechanisms of necroptosis: an ordered cellular explosion, Nat. Rev. Mol. Cell Biol. 11 (2010) 700–714.
[18] R. Weinlich, C.P. Dillon, D.R. Green, Ripped to death, Trends Cell Biol. 21 (2011) 630–637.
[19] L. Galluzzi, G. Kroemer, Necroptosis: a specialized pathway of programmed necrosis, Cell 135 (2008) 1161–1163.
[20] P. Golstein, G. Kroemer, Cell death by necrosis: towards a molecular definition, Trends Biochem. Sci. 32 (2007) 37–43.
[21] N. Vanlangenakker, T. Vanden Berghe, D. Krysko, N. Festjens, P. Vandenabeele, Molecular mechanisms and pathophysiology of necrotic cell death, Curr. Mol. Med. 8 (2008) 207–220.
[22] G. Kroemer, L. Galluzzi, P. Vandenabeele, J. Abrams, E.S. Alnemri, E.H. Baehrecke, M.V. Blagosklonny, W.S. El-Deiry, P. Golstein, D.R. Green, M. Hengartner, R.A. Knight, S. Kumar, S.A. Lipton, W. Malorni, G. Nuñez, M.E. Peter, J. Tschopp, J. Yuan, M. Piacentini, B. Zhivotovsky, G. Melino, Classification of cell death: recommendations of the nomenclature committee on cell death 2009, Cell Death Differ. 16 (2009) 3–11.
[23] U. Ziegler, P. Groscurth, Morphological features of cell death, Physiology 19 (2004) 124–128.
[24] N. Festjens, T. Vanden Berghe, S. Cornelis, P. Vandenabeele, RIP1, a kinase on the crossroads of a cell's decision to live or die, Cell Death Differ. 14 (2007) 400–410.
[25] G. Neves, C.B. Antonio, A.H. Betti, M.A. Pranke, C.A.M. Fraga, E.J. Barreiro, F. Noël, S.M.K. Rates, New insights into pharmacological profile of LASSBio-579, a multitarget *N*-phenylpiperazine derivative active on animal models of schizophrenia, Behav. Brain Res. 237 (2013) 86–95.
[26] R. Hubrecht, J. Kirkwood, The UFAW Handbook on the Care and Management of Laboratory and Other Research Animals, 8th ed., Wiley-Blackwell, United Kingdom, 2010.
[27] T.E.T. Pompeu, F.R.S. Alves, C.D.M. Figueiredo, C.B. Antonio, V. Herzfeldt, B.C. Moura, S.M.K. Rates, E.J. Barreiro, C.A.M. Fraga, F. Noël, Synthesis and pharmacological evaluation of new *N*-phenylpiperazine derivatives designed as homologues of the antipsychotic lead compound LASSBio-579, Eur. J. Med. Chem. 66 (2013) 122–134.
[28] M.F. Mota, P.L. Benfica, A.C. Batista, F.S. Martins, J.R. de Paula, M.C. Valadares, Investigation of Ehrlich ascites tumor cell death mechanisms induced by *Synadenium umbellatum* Pax, J. Ethnopharmacol. 139 (2012) 319–329.
[29] T. Mosmann, Rapid colorimetric assay for cellular growth and survival: application to proliferation and cytotoxicity assays, J. Immunol. Methods 65 (1983) 55–63.
[30] C. Hellerbrand, E. Bumes, F. Bataille, W. Dietmaier, R. Massoumi, A.K. Bosserhoff, Reduced expression of CYLD in human colon and hepatocellular carcinomas, Carcinogenesis 28 (2007) 21–27.
[31] K.-C. Cheng, H.-C. Huang, J.-H. Chen, J.-W. Hsu, H.-C. Cheng, C.-H. Ou, W.-B. Yang, S.-T. Chen, C.-H. Wong, H.-F. Juan, *Ganoderma lucidum* polysaccharides in human monocytic leukemia cells: from gene expression to network construction, BMC Genomics 8 (2007) 411-411.
[32] U.J. Lee, S.-R. Choung, K.V.B. Prakash, E.-J. Lee, M.Y. Lee, Y.J. Kim, C.-W. Han, Y.-C. Choi, Dual knockdown of p65 and p50 subunits of NF-kappaB by siRNA inhibits the induction of inflammatory cytokines and significantly enhance apoptosis in human primary synoviocytes treated with tumor necrosis factor-alpha, Mol. Biol. Rep. 35 (2008) 291–298.
[33] H.-W. Rho, B.-C. Lee, E.-S. Choi, I.-J. Choi, Y.-S. Lee, S.-H. Goh, Identification of valid reference genes for gene expression studies of human stomach cancer by reverse transcription-qPCR, BMC Cancer 10 (2010) 240-240.
[34] M.W. Pfaffl, A new mathematical model for relative quantification in real-time RT–PCR, Nucleic Acids Res. 29 (2001) e45-e45.
[35] A. Pessina, B. Albella, J. Bueren, P. Brantom, S. Casati, L. Gribaldo, C. Croera, G. Gagliardi, P. Foti, R. Parchment, D. Parent-Massin, Y. Sibiril, R. Van Den Heuvel, Prevalidation of a model for predicting acute neutropenia by colony forming unit granulocyte/macrophage (CFU-GM) assay, Toxicol. In Vitro 15 (2001) 729–740.
[36] ICCVAM, Test Method Evaluation Report (TIMER): *In Vitro* Cytotoxicity Test Methods for Estimating Starting Doses for Acute Oral Systemic Toxicity Test, NIH Publication no. 07-4519. Research Triangle Park, NC: National Institute for Environmental Health Sciences, 2006.
[37] M.S. Vieira, V. de Oliveira, E.M. Lima, M.J. Kato, M.C. Valadares, *In vitro* basal cytotoxicity assay applied to estimate acute oral systemic toxicity of grandisin and its major metabolite, Exp. Toxicol. Pathol. 63 (2011) 505–510.
[38] OECD, Acute Oral Toxicity - Acute Toxic Class Method, Test no. 423 OECD Publishing, 2001.
[39] M. Malone, New natural products and plant drugs with pharmacological, biological or therapeutical activity, Pharmacological Approaches to Natural Product, Screening and Evaluation, (1977).
[40] C. Giampietri, D. Starace, S. Petrungaro, A. Filippini, E. Ziparo, Necroptosis: molecular signalling and translational implications, Int. J. Cell Biol. 2014 (2014) 6.
[41] S.W.G. Tait, G. Ichim, D.R. Green, Die another way – non-apoptotic mechanisms of cell death, J. Cell Sci. 127 (2014) 2135–2144.
[42] M. Kawase, N. Motohashi, T. Kurihara, M. Inagaki, K. Satoh, H. Sakagami, Relationship between radical intensity and cytotoxic activity of dopamine-related compounds, Anticancer Res. 18 (1998) 1069–1074.
[43] Q. He, L. Yuan, Dopamine inhibits proliferation, induces differentiation and apoptosis of K562 leukaemia cells, Chin. Med. J. (Engl.) 120 (2007) 970–974.
[44] M. Wick, 3,4-Dihydroxybenzylamine: a dopamine analog with enhanced antitumor activity against B16 melanoma, J. Natl. Cancer Inst. (63) (1979) 1465–1467.
[45] T. Pollmacher, D. Hinze-Selch, J. Mullington, Effects of clozapine on plasma cytokine and soluble cytokine receptor levels, J. Clin. Psychopharmacol. 16 (1996) 403–409.
[46] N.A. Massari, V.A. Medina, G.P. Cricco, D.J. Martinel Lamas, L. Sambuco, R. Pagotto, C. Ventura, P.J. Ciraolo, O. Pignataro, R.M. Bergoc, E.S. Rivera, Antitumor activity of histamine and clozapine in a mouse experimental model of human melanoma, J. Dermatol. Sci. 72 (2013) 252–262.
[47] S. Suzuki, M. Okada, K. Kuramoto, H. Takeda, H. Sakaki, H. Watarai, T. Sanomachi, S. Seino, T. Yoshioka, C. Kitanaka, Aripiprazole, an antipsychotic and partial dopamine agonist, inhibits cancer stem cells and reverses chemoresistance, Anticancer Res. 36 (2016) 5153–5161.
[48] T.V. Berghe, A. Linkermann, S. Jouan-Lanhouet, H. Walczak, P. Vandenabeele, Regulated necrosis: the expanding network of non-apoptotic cell death pathways, Nat. Rev. Mol. Cell Biol. 15 (2014) 135–147.
[49] L. Galluzzi, O. Kepp, S. Krautwald, G. Kroemer, A. Linkermann, Molecular mechanisms of regulated necrosis, Semin. Cell Dev. Biol. 35 (2014) 24–32.
[50] S. Fulda, The mechanism of necroptosis in normal and cancer cells, Cancer Biol. Ther. 14 (2013) 999–1004.
[51] D.E. Christofferson, J. Yuan, Necroptosis as an alternative form of programmed cell death, Curr. Opin. Cell Biol. 22 (2010) 263–268.
[52] S. McComb, H.H. Cheung, R.G. Korneluk, S. Wang, L. Krishnan, S. Sad, cIAP1 and cIAP2 limit macrophage necroptosis by inhibiting Rip1 and Rip3 activation, Cell Death Differ. 19 (2012) 1791–1801.
[53] M.A. O'Donnell, E. Perez-Jimenez, A. Oberst, A. Ng, R. Massoumi, R. Xavier, D.R. Green, A.T. Ting, Caspase 8 inhibits programmed necrosis by processing CYLD, Nat. Cell Biol. 13 (2011) 1437–1442.
[54] A. Kaczmarek, O. Krysko, L. Heyndrickx, T. Løve Aaes, T. Delvaeye, C. Bachert, L. Leybaert, P. Vandenabeele, D.V. Krysko, TNF/TNF-R1 pathway is involved in doxorubicin-induced acute sterile inflammation, Cell Death Dis. 4 (2013) e961.
[55] Y. Dondelinger, M. Darding, M.J.M. Bertrand, H. Walczak, Poly-ubiquitination in TNFR1-mediated necroptosis, Cell. Mol. Life Sci. 73 (2016) 2165–2176.
[56] Y. Assef, F. Rubio, G. Coló, S. del Mónaco, M.A. Costas, B.A. Kotsias, Imatinib resistance in multidrug-resistant K562 human leukemic cells, Leuk. Res. 33 (2009) 710–716.
[57] T. Braun, G. Carvalho, C. Fabre, J. Grosjean, P. Fenaux, G. Kroemer, Targeting NF-[kappa]B in hematologic malignancies, Cell Death Differ. 13 (2006) 748–758.
[58] D. Cilloni, F. Messa, F. Arruga, I. Defilippi, A. Morotti, E. Messa, S. Carturan, E. Giugliano, M. Pautasso, E. Bracco, V. Rosso, A. Sen, G. Martinelli, M. Baccarani, G. Saglio, The NF-[kappa]B pathway blockade by the IKK inhibitor PS1145 can overcome imatinib resistance, Leukemia 20 (2005) 61–67.
[59] A. Oeckinghaus, M.S. Hayden, S. Ghosh, Crosstalk in NF-[kappa]B signaling pathways, Nat. Immunol. 12 (2011) 695–708.
[60] D. Kirchner, J. Duyster, O. Ottmann, R.M. Schmid, L. Bergmann, G. Munzert, Mechanisms of Bcr-Abl-mediated NF-kappaB/Rel activation, Exp. Hematol. 31 (2003) 504–511.
[61] S. Sakon, X. Xue, M. Takekawa, T. Sasazuki, T. Okazaki, Y. Kojima, J.-H. Piao, H. Yagita, K. Okumura, T. Doi, H. Nakano, NF-κB inhibits TNF-induced accumulation of ROS that mediate prolonged MAPK activation and necrotic cell death, EMBO J. 22 (2003) 3898–3909.
[62] R.J. Thapa, S.H. Basagoudanavar, S. Nogusa, K. Irrinki, K. Mallilankaraman, M.J. Slifker, A.A. Beg, M. Madesh, S. Balachandran, NF-κB protects cells from gamma interferon-induced RIP1-dependent necroptosis, Mol. Cell. Biol. 31 (2011) 2934–2946.
[63] J. Hitomi, D.E. Christofferson, A. Ng, J. Yao, A. Degterev, R.J. Xavier, J. Yuan, Identification of a molecular signaling network that regulates a cellular necrotic cell death pathway by a genome wide siRNA screen, Cell 135 (2008) 1311–1323.
[64] S. He, L. Wang, L. Miao, T. Wang, F. Du, L. Zhao, X. Wang, Receptor interacting protein kinase-3 determines cellular necrotic response to TNF-α, Cell 137 (2009) 1100–1111.
[65] N. Vanlangenakker, T. Vanden Berghe, P. Bogaert, B. Laukens, K. Zobel, K. Deshayes, D. Vucic, S. Fulda, P. Vandenabeele, M.J.M. Bertrand, cIAP1 and TAK1 protect cells from TNF-induced necrosis by preventing RIP1/RIP3-dependent reactive oxygen species production, Cell Death Differ. 18 (2011) 656–665.
[66] D. Vercammen, R. Beyaert, G. Denecker, V. Goossens, G. Van Loo, W. Declercq, J. Grooten, W. Fiers, P. Vandenabeele, Inhibition of caspases increases the sensitivity of L929 cells to necrosis mediated by tumor necrosis factor, J. Exp. Med. 187 (1998) 1477–1485.
[67] A. Degterev, Z. Huang, M. Boyce, Y. Li, P. Jagtap, N. Mizushima, G.D. Cuny, T.J. Mitchison, M.A. Moskowitz, J. Yuan, Chemical inhibitor of nonapoptotic cell death with therapeutic potential for ischemic brain injury, Nat. Chem. Biol. 1 (2005) 112–119.
[68] K.D. Marshall, C.P. Baines, Necroptosis: is there a role for mitochondria? Front. Physiol. 5 (2014) 323.
[69] K. Banki, E. Hutter, N.J. Gonchoroff, A. Perl, Elevation of mitochondrial transmembrane potential and reactive oxygen intermediate levels are early events and occur independently from activation of caspases in Fas signaling, J. Immunol. 162 (1999) 1466–1479.
[70] T.V. Berghe, N. Vanlangenakker, E. Parthoens, W. Deckers, M. Devos, N. Festjens, C.J. Guerin, U.T. Brunk, W. Declercq, P. Vandenabeele, Necroptosis, necrosis and secondary necrosis converge on similar cellular disintegration features, Cell Death Differ. 17 (2010) 922–930.
[71] V. Goossens, K.D. Vos, D. Vercammen, M. Steemans, K. Vancompernolle, W. Fiers, P. Vandenabeele, J. Grooten, Redox regulation of TNF signaling, BioFactors 10 (1999) 145–156.
[72] D. Han, M.D. Ybanez, S. Ahmadi, K. Yeh, N. Kaplowitz, Redox regulation of tumor necrosis factor signaling, Antioxid. Redox Signal. 11 (2009) 2245–2263.

[73] W. Chen, Z. Zhou, L. Li, C.-Q. Zhong, X. Zheng, X. Wu, Y. Zhang, H. Ma, D. Huang, W. Li, Z. Xia, J. Han, Diverse sequence determinants control human and mouse receptor interacting protein 3 (RIP3) and mixed lineage kinase domain-like (MLKL) interaction in necroptotic signaling, J. Biol. Chem. 288 (2013) 16247–16261.

[74] A. Pessina, E. Turlizzi, A. Bonomi, F. Guizzardi, L. Cavicchini, C. Croera, S. Bareggi, *In vitro* toxicity of clozapine, olanzapine, and quetiapine on granulocyte-macrophage progenitors (GM-CFU), Pharmacopsychiatry 39 (2006) 20–22.

[75] S. Kurtin, Myeloid toxicity of cancer treatment, J. Adv. Pract. Oncol. 3 (2012) 209–224.

[76] G. Rosenfeld, Pancromic staining for clinical hematology and citology: a novel combination of may-grunwald and giemsa components in one rapid usage staining, Mem. Inst. Butantan 20 (1947) 329–335.

[77] I.L. Finar, K.E. Godfrey, The preparation and properties of some derivatives of 1-phenylpyrazole, J. Chem. Soc. (1954) 2293–2298.